Evaluating vegetation change in a subarctic catchment through fusion of remotely sensed data

Sean Leipe, M.Sc Candidate

School of Geography & Earth Sciences

McMaster University

1. Introduction

High-latitude ecosystems have experienced substantial warming over the past 40 years [1, 2, 3], causing an increase in vegetation growth throughout the circumpolar North [4, 5]. A major component of this change is shrub expansion in arctic and subarctic ecotones [5, 6]. The rates of shrub expansion are highly variable depending on plant species, topographic position, hydrology, soils, and other ecosystem properties [6]. Changes in shrub and other vegetation properties are critical to document due to their first-order control on water, energy and carbon balances [5]. Understanding these changes is critical for predicting the future of northern watersheds under a rapidly changing climate. This study uses multi-temporal airborne LiDAR, optical imagery, and field methods to quantify shrub expansion over 11 years in a well-studied subarctic mountain basin.

2. Study Area

This study was conducted in the Granger Basin, a ~7.6km^2 subarctic headwater catchment located in the Wolf Creek Research Basin (WCRB) [7] (Figure 1). The WCRB is a 180km^2 long-term watershed research facility located ~15km south of Whitehorse, Yukon Territory [8]. Granger Basin straddles the WCRB's subalpine and alpine tundra ecozones, with an elevation range of 1356 to 2080 m.a.s.l. and a subarctic-continental climate [9]. While both the overall WCRB and Granger Basin have over 20 years of comprehensive meteorological data on record [10], there remains a lack of research on its vegetation and its influence on the hydrological cycle.

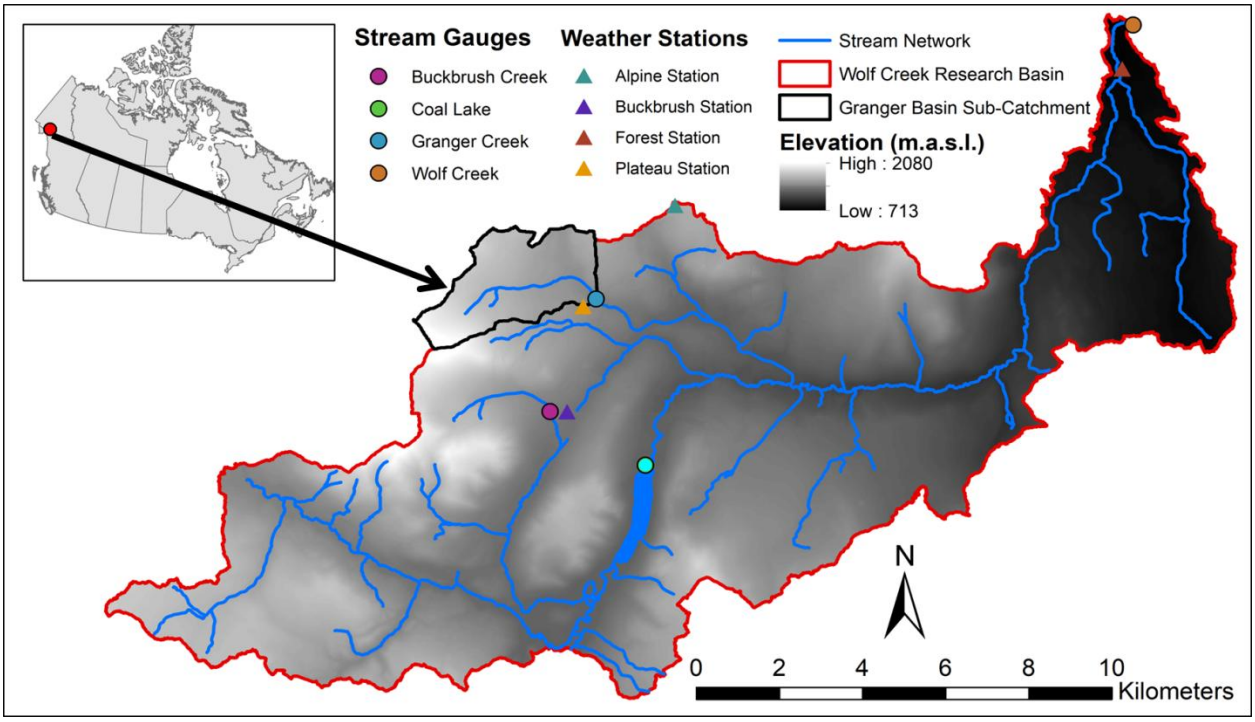

Figure 1: LiDAR DEM of the WCRB along with selected long-term monitoring sites

3. Field Methodology

29 vegetation transects were spread throughout Granger Basin (Figure 2) to evaluate shrub properties for comparisons to the LiDAR. Transects were located on slopes with a consistent aspect and obvious shrub presence as interpreted from LiDAR and pan-sharpened Worldview-2 imagery.

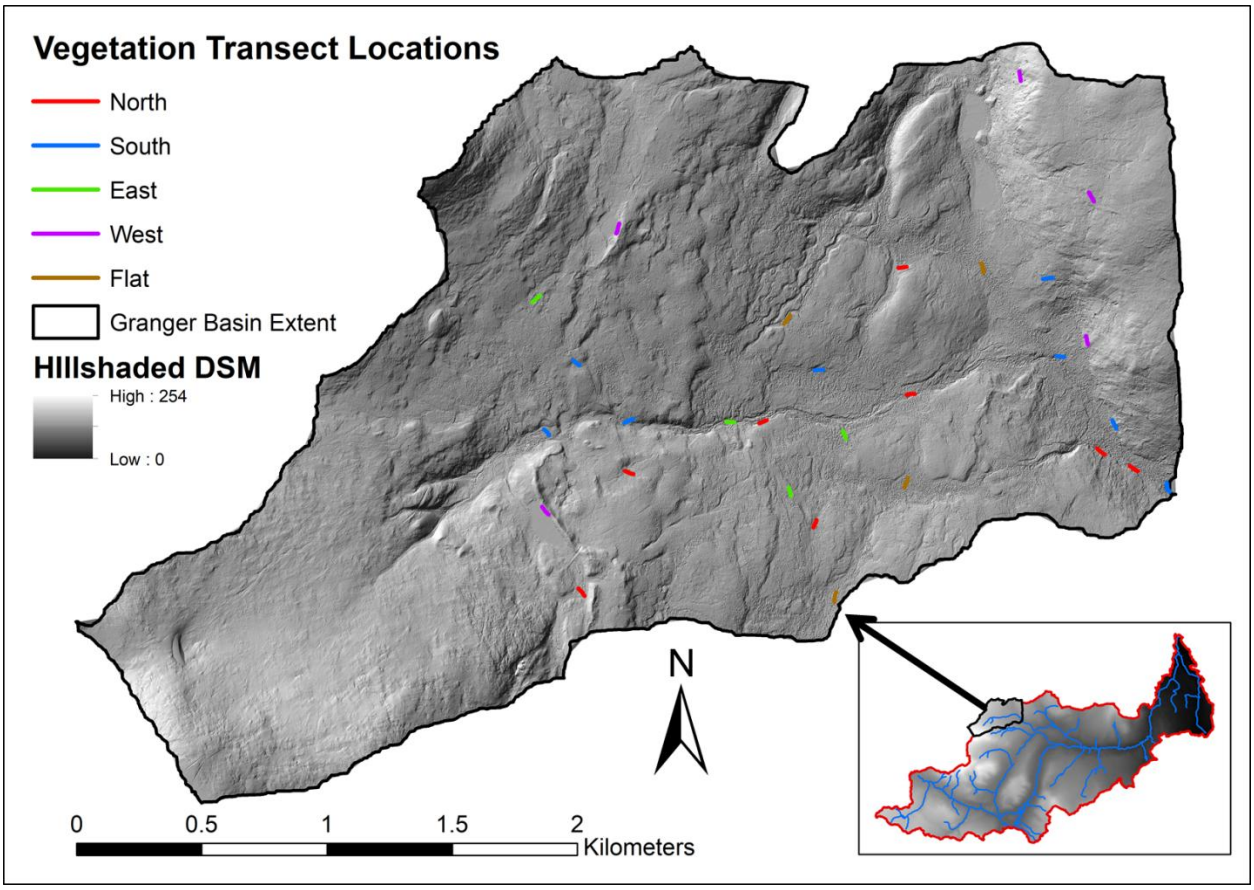

Figure 2: Location of vegetation transects within Granger Basin, classified by dominant aspect

These target sites were navigated to in the field using the Collector for ArcGIS mobile application. Each 40m transect consisted of 5 circular plots with a 1m radius, spaced out at every 10m (Figure 3). Field measurements were appended to differential GPS coordinates of plot centroids in R Statistics and used to create new plot area shapefiles through the R-ArcGIS Bridge and ArcPy.

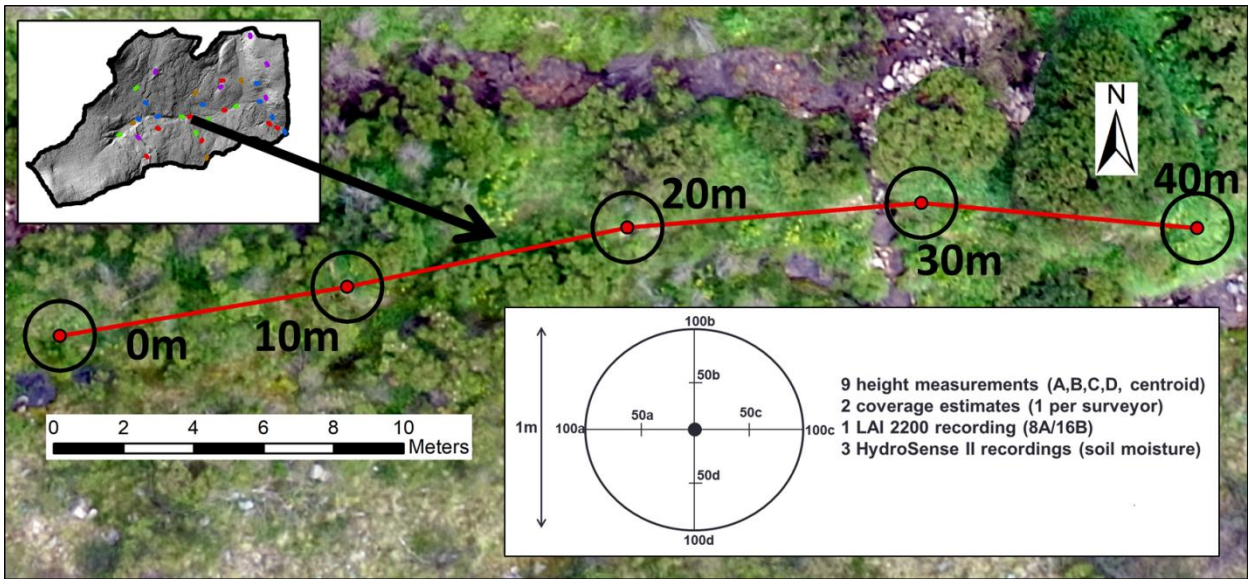

Figure 3: Example vegetation transect in Granger Basin along with diagram of survey methodology

4. LiDAR Processing

Airborne LiDAR surveys of the WCRB were conducted in August 2007 (return density = 0.67/ m^2) and August 2018 (return density = 11/ m^2). As lower sampling rates make LiDAR pulses more likely to miss the highest points of vegetation and underestimate heights compared to field measurements [11], these differences in survey resolutions had to be accounted for. The 2018 point cloud was thinned to an average density of 0.67/m^2 to match with 2007 by randomly retaining a specified fraction of its original returns. Once all point clouds were pre-processed and height-normalized through LAStools batch scripting [12], height-above-ground (HAG) metrics were extracted for each plot radius (Figure 4). These were compared to field measurements to evaluate how well the LiDAR surveys could estimate plot vegetation heights, with the goal of evaluating changes in height over time. As LiDAR tends to display high levels of shrub height underestimation compared to field measurements [13], LAS return heights were compared to both the maximum and average heights measured in each plot.

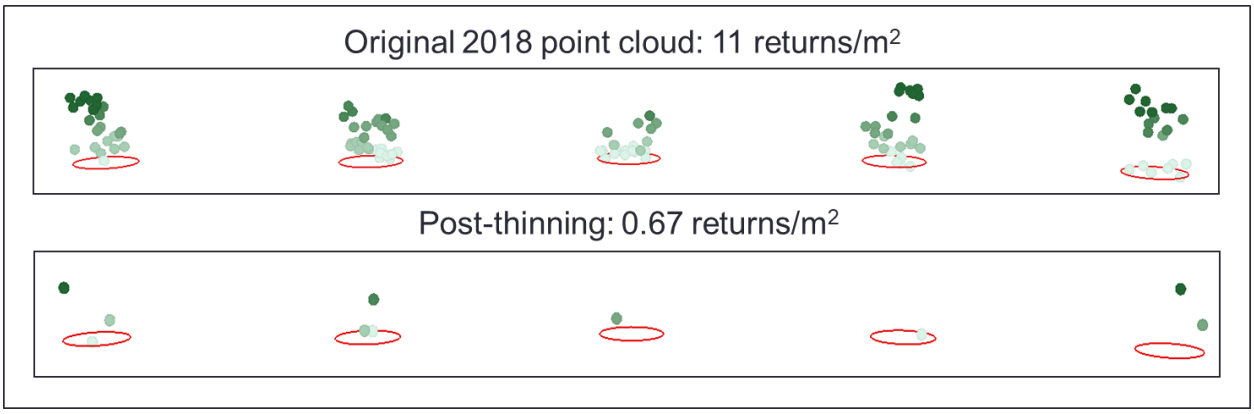

Figure 4: 2018 LiDAR HAG metrics extracted for same transect as Fig. 3, before and after thinning

The ability of the 2018 survey to model shrub presence and absence was also explored. Binary supervised classifications based on LiDAR metrics were conducted through the Random Forests (RF) machine learning classifier in R Statistics [14], using field data for model training and validation. Predictors included in the best-performing classification are shown in Table 1:

Table 1: LiDAR-derived variables used as predictors in the best-performing RF model, all created as rasters with 2m spatial resolution using a 3x3 focal moving window

Variable	**Description**	**Source**
Average HAG	Average LAS return height	Height-normalized point cloud
Maximum HAG	Maximum LAS return height	Height-normalized point cloud
SD of HAG	Standard deviation of LAS return heights	Height-normalized point cloud
Vegetation Return Count	Total number of LAS returns >45cm above ground surface	Height-normalized point cloud
Vegetation Return Density	Ratio of LAS returns >45cm above ground surface to total number of returns	Height-normalized point cloud
DEM	Elevation surface interpolated from ground returns	Ground-classified point cloud (with original z-values)

The model with highest independent accuracy using the thinned 2018 point cloud was applied to the 2007 LiDAR to create raster layers of shrub cover for both years, which were exported using the R-ArcGIS Bridge. By subtracting the 2007 layer from 2018 in the Raster Calculator, a new change layer was created where pixel values of 1 = shrub growth, 0 = no change, and -1 = shrub loss.

5. Results

The original high-density 2018 point cloud was found to underestimate maximum field-measured heights within the 1m plots by only 11cm on average, with an overall R^2 of 0.79 (Figure 5).

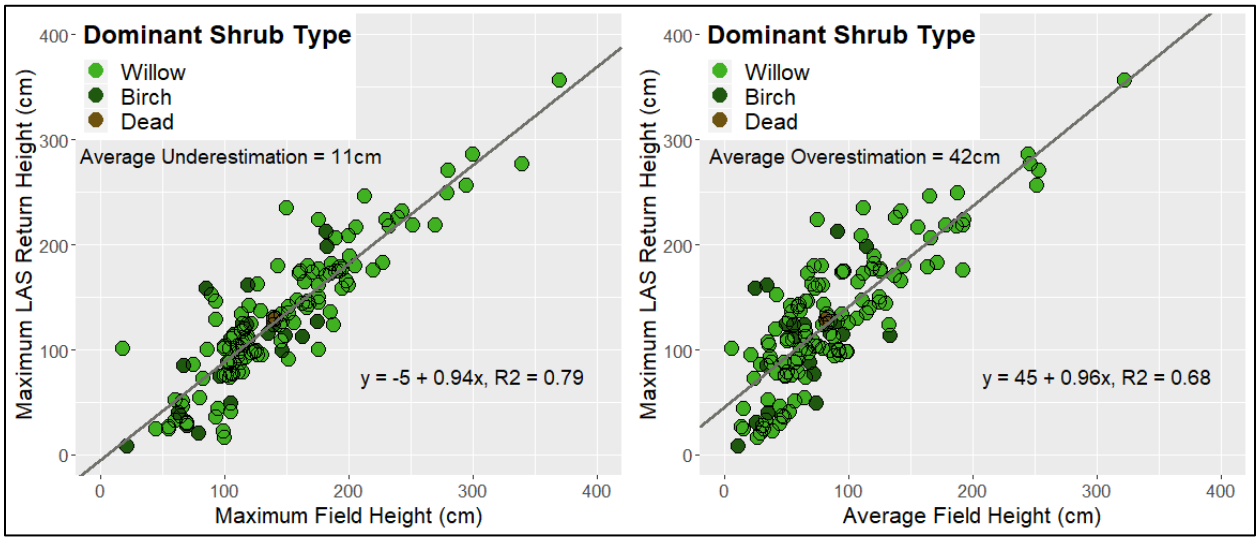

Figure 5: Original 2018 LAS metrics compared to shrub heights from field plots

Thinning the point cloud substantially decreased accuracy across the board, most likely from increased sampling error as a result of its lower return density [15]. Maximum heights within the plots were underestimated by 60cm after thinning, with an R^2 of only 0.47 (Figure 6).

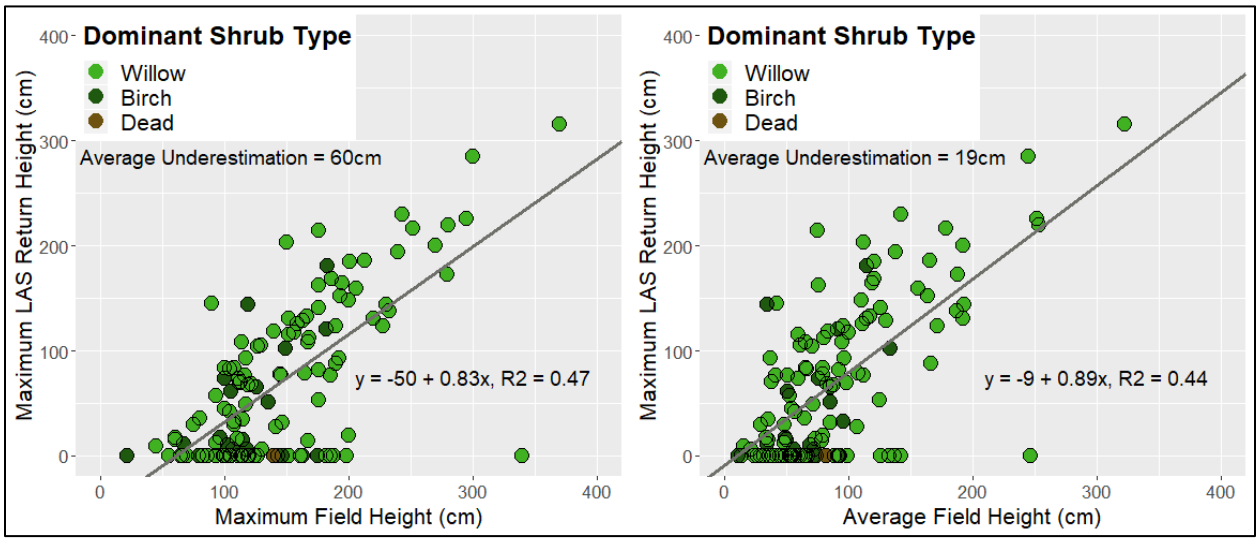

Figure 6: Thinned 2018 LAS metrics compared to shrub heights from field plots

Due to these high levels of height underestimation, binary presence and absence models for the thinned 2018 LiDAR were used instead to evaluate change. The best-performing classification predicted shrub presence/absence in 2018 with 93% overall independent accuracy.

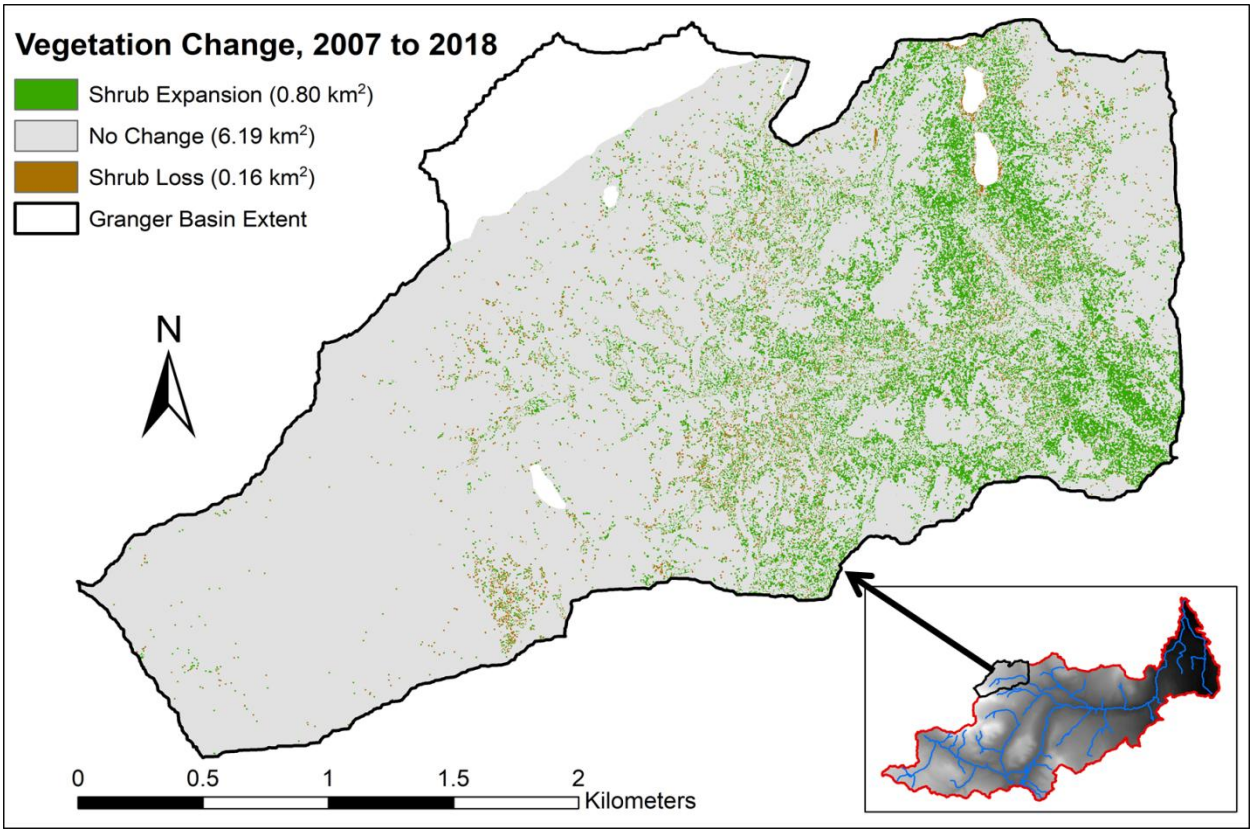

Figure 7: Changes in LiDAR-derived shrub cover models between 2007 and 2018 surveys

The change layer created by subtracting the 2007 shrub cover layer from 2018 (Figure 7) shows clear and substantial increases in shrub cover throughout the lower basin, with expansion in over 11% of the total area covered by both LiDAR surveys. The majority of misclassified pixels exist around lakes/ponds with varying extents between survey years and rock fields in the upper basin that resemble shrubs in terms of the RF model predictors.

6. Conclusion

Airborne LiDAR was used along with optical imagery and field surveys to evaluate vegetation change over time in a well-studied subarctic mountain basin. Though low return densities led to inaccurate vegetation height estimates, LiDAR was successfully used to predict shrub presence and absence with high accuracy and evaluate changes in cover over the 11 years between surveys. Results show clear increases in vegetation cover throughout the study area between 2007 and 2018. Future work will quantitatively compare these changes across landscape properties such as elevation, slope, aspect, and other topographic indices.

7. Acknowledgements

I would like to thank my supervisor Dr. Sean Carey for his mentorship and support; Dr. Chris Hopkinson & Allyson Fox from AGRG for the 2007 LiDAR survey and Dr. Brian Menounos from UNBC for the 2018 LiDAR survey; David Barrett, Tyler de Jong, Joseph Desmarais, Fiona Chapman, Erin Nicholls, & Nadine Shatilla from the McMaster Watershed Hydrology Group for support in the field; and the Global Water Futures program for providing funding that made this work possible.

8. References

1. Hinzman, L. D., Bettez, N. D., Bolton, W. R., Chapin, F. S., Dyurgerov, M. B., Fastie, C. L., … Yoshikawa, K. (2005). Evidence and implications of recent climate change in Northern Alaska and other Arctic regions. *Climatic Change, 72*(3), 251–298.

2. Overpeck, J., Hughen, K., Hardy, D., Bradley, R., Case, R., Douglas, M., … Zielinski, G. (1997). Arctic environmental change of the last four centuries. *Science, 278*(5341), 1251–1256.

3. Tape, K., Sturm, M., & Racine, C. (2006). The evidence for shrub expansion in Northern Alaska and the Pan-Arctic. *Global Change Biology*, *1*(2), 686–702.

4. Myers-Smith, I. H., Forbes, B. C., Wilmking, M., Hallinger, M., Lantz, T., Blok, D., … Hik, D. S. (2011). Shrub expansion in tundra ecosystems: Dynamics, impacts and research priorities. *Environmental Research Letters*, *6*(4).

5. Epstein, H. E., Myers-Smith, I., & Walker, D. A. (2013). Recent dynamics of arctic and sub-arctic vegetation. *Environmental Research Letters*, *8*(1).

6. Tape, K. D., Hallinger, M., Welker, J. M., & Ruess, R. W. (2012). Landscape Heterogeneity of Shrub Expansion in Arctic Alaska. *Ecosystems*, *15*(5), 711–724.

6. Carey, S. K., Boucher, J. L., & Duarte, C. M. (2013). Inferring groundwater contributions and pathways to streamflow during snowmelt over multiple years in a discontinuous permafrost subarctic environment (Yukon, Canada). *Hydrogeology Journal, 21*(1), 67–77.

8. Janowicz, J. R. (1999). Wolf Creek Research Basin – Overview. *Department of Indian and Northern Affairs Canada.*

9. McCartney, S. E., Carey, S. K., & Pomeroy, J. W. (2006). Intra-basin variability of snowmelt water balance calculations in a subarctic catchment. *Hydrological Processes, 20*(4), 1001–1016.

10. Rasouli, K., Pomeroy, J. W., Janowicz, J. R., Williams, T. J., and Carey, S. K. (2019). A long-term hydrometeorological dataset (1993– 2014) of a northern mountain basin: Wolf Creek Research Basin, Yukon Territory, Canada. *Earth System Science Data, 11*, 89–100.

11. Zhao, K., Suarez, J. C., Garcia, M., Hu, T., Wang, C., & Londo, A. (2018). Utility of multitemporal lidar for forest and carbon monitoring: Tree growth, biomass dynamics, and carbon flux. *Remote Sensing of Environment*, *204*(September 2016), 883–897.

12. Isenburg, M. (2019). LAStools - efficient tools for LiDAR processing. Version 190927, http://lastools.org

13. Hopkinson, C., Chasmer, L. E., Sass, G., Creed, I. F., Sitar, M., Kalbfleisch, W., & Treitz, P. (2005). Vegetation class dependent errors in lidar ground elevation and canopy height estimates in a boreal wetland environment. *Canadian Journal of Remote Sensing*, *31*(2), 191–206.

14. Liaw, A., & Wiener, M. (2002). Classification and Regression by randomForest. *R News*, *2*(December), 18–22.

15. Streutker, D. R., & Glenn, N. F. (2006). LiDAR measurement of sagebrush steppe vegetation heights. *Remote Sensing of Environment*, *102*(1–2), 135–145.